



Available online at www.sciencedirect.com

ScienceDirect

Journal of Nutritional Biochemistry

Journal of Nutritional Biochemistry 146 (2025) 110039

RESEARCH PAPER

Lactoferrin attenuates renal fibrosis and uremic sarcopenia in a mouse model of adenine-induced chronic kidney disease

Yukina Iwamoto^a, Seiko Yamakoshi^a, Akiyo Sekimoto^a, Koji Hosomi^{b,c}, Takashi Toyama^d, Yoshiro Saito^d, Jun Kunisawa^{b,e,f,g,h,i,j,k}, Nobuyuki Takahashi^{a,l}, Eikan Mishima^{l,m,n}, Emiko Sato^{a,l,*}

^a Division of Clinical Pharmacology and Therapeutics, Graduate School of Pharmaceutical Sciences, Tohoku University, Sendai, 980-8578, Japan
^b Laboratory of Vaccine Materials and Laboratory of Gut Environmental System, Microbial Research Center for Health and Medicine, National Institutes of Biomedical Innovation,

Health and Nutrition [NIBN], Osaka, 567-0085, Japan

^c Graduate School of Veterinary Science, Osaka Metropolitan University, Izumisano, 598-8531, Japan
^d Laboratory of Molecular Biology and Metabolism, Graduate School of Pharmaceutical Sciences, Tohoku University, Sendai, 980-8578, Japan
^e Graduate School of Medicine, Osaka University, 565-0871, Suita, Japan

Graduate School of Medicine, Osaka University, 305-0871, Suita, Japan

Graduate School of Pharmaceutical Sciences, Osaka University, Suita, 565-0871, Japan

Graduate School of Dentistry, Osaka University, Suita, 565-0871, Japan

Graduate School of Science, Osaka University, Toyonaka, 560-0043, Japan

¹International Vaccine Design Center, The Institute of Medical Science, The University of Tokyo, Minato-ku, 108-8639, Japan

¹Department of Microbiology and Immunology, Kobe University Graduate School of Medicine, Kobe, 657-8501, Japan

^k Research Organization for Nano and Life Innovation, Waseda University, Shinjuku-ku, 162-0041, Japan

¹Department of Nephrology, Tohoku University Graduate School of Medicine, 980-8575, Sendai, Japan

^m Department of Redox Molecular Medicine, Tohoku University Graduate School of Medicine, Sendai 980-8575, Japan

ⁿ Institute of Metabolism and Cell Death, Helmholtz Zentrum München, Neuherberg, 85764, Germany

Received 14 April 2025; received in revised form 18 July 2025; accepted 22 July 2025

Abstract

The prevalence of chronic kidney disease (CKD) continues to rise, highlighting the urgent need for effective therapeutic interventions to address its various complications including sarcopenia. Lactoferrin, a multifunctional iron-binding glycoprotein found in mammalian breast milk, exhibits various biological activities and holds potential for treating CKD and its complications. This study investigated the effects of lactoferrin on CKD progression, its complications, and underlying mechanisms. A mouse model of adenine-induced renal failure was used as a CKD model. Lactoferrin was administered during the same period as adenine administration to assess its preventative effect on the progression of CKD. In another experiment, lactoferrin was administered after the adenine administration period to examine its effect on already advanced CKD. Effects of lactoferrin on renal function, renal pathology, and muscle atrophy were evaluated. Additionally, mechanistic insights were explored through mRNA and protein expression profiling, gut microbiota characterization, and metabolomic analysis. Lactoferrin administration improved reduction of renal function, and mitigated renal atrophy, and tubulointerstitial damage, and ameliorated skeletal muscle atrophy in CKD mice. In the skeletal muscle, CKD induced aberrant activation of mTOR1, impaired autophagy, and disrupted branched-chain amino acid metabolism. This abnormal activation of the proteolysis pathways was ameliorated by lactoferrin. Furthermore, lactoferrin attenuated dysbiosis-induced production of microbiota-derived uremic toxins, thereby reducing the indoxyl sulfate accumulation in blood and muscle. These effects contributed to decreased renal damage and delayed sarcopenia progression. Collectively, these findings suggest that lactoferrin may serve as a promising preventive and therapeutic agent for CKD-associated sarcopenia via the gut-kidney-skeletal muscle axis.

© 2025 The Authors. Published by Elsevier Inc.

This is an open access article under the CC BY license (http://creativecommons.org/licenses/by/4.0/)

Keywords: Chronic kidney disease; Lactoferrin; Uremic sarcopenia; Uremic toxin; Metabolomics.

Abbreviations: CKD, chronic kidney disease; Lf, lactoferrin; BUN, blood urea nitrogen.

^{*} Corresponding author at: Aoba 6-3, Aramaki, Aoba-ku, Sendai, Miyagi 980-8578, Japan. *E-mail address*: emiko.sato.b8@tohoku.ac.jp (E. Sato).

1. Introduction

Chronic kidney disease (CKD), a condition characterized by gradual decline of kidney function over time, is a global health challenge and is associated with numerous serious complications. Sarcopenia, characterized by the progressive and generalized loss of muscle strength and mass, has gained increasing recognition as an important complication in patients with CKD, particularly those with end-stage kidney disease [1–3]. Sarcopenia is associated with progression of CKD [4], increasing frailty [5,6], higher mortality rates [7,8] and reduced quality of life in patients with CKD. However, the pathogenesis of sarcopenia in CKD remains incompletely understood, and no established prevention or treatment strategies currently exist.

Patients with CKD are susceptible to sarcopenia due to increased oxidative stress, metabolic disturbances, and enhanced muscle protein catabolism driven by uremia [9–12]. Uremic toxins, harmful metabolites that accumulate in the body due to impaired renal function in CKD, are implicated in a variety of biological disorders. We have reported that the uremic toxins accumulate in systemic organs such as kidney, brain and, muscle, exerting adverse effects [13]. For instance, indoxyl sulfate, a representative uremic toxin, has been linked to CKD complications, including sarcopenia through mechanisms involving inflammation, oxidative stress, and metabolic dysregulation [14,15]. Of note, key uremic toxins, such as indoxyl sulfate and hippuric acid, are produced by the gut microbiota metabolism [16–18]. Thus, dysbiosis of the gut microbiota has been shown to exacerbate uremic toxin production and contribute to CKD progression through the gut-kidney axis [17,19].

Lactoferrin, an iron-binding multifunctional glycoprotein and member of the transferrin family, is found in mammalian milk, tears, saliva, cerebrospinal fluid, and other excretory fluids [20]. It plays a vital role in innate immunity, exhibiting antibacterial, anti-inflammatory, and immunomodulatory properties [21]. Lactoferrin has been reported to demonstrate renoprotective effect against acute kidney injury [22], and improvements in intestinal environment [23–26]. Despite these promising findings, the role of lactoferrin in CKD and its associated complications, particular sarcopenia, remains unclear. This study investigates the effects of lactoferrin on CKD progression and sarcopenia and explores the underlying mechanisms using a mouse model of adenine-induced CKD.

2. Experimental section

2.1. Animal studies

All animal experiments were approved by the Animal Committee of Tohoku University (Approval No. 2019PhA-010, 15 Feb 2019). Experimental protocols and animal care were performed according to the guidelines for the care and use of animals established by Tohoku University and have been performed in accordance with the ethical standards laid down in the 1964 Declaration of Helsinki and its later amendments. Male C57BL/6JJcl mice of 7 weeks of age were purchased from CLEA Japan, Inc. (Tokyo, Japan). Animals were housed at 24°C on a 12:12 h light-dark cycle and fed a regular chow (MF, Oriental Yeast Co., ltd, Tokyo, Japan) and water at libitum. At eight weeks of age, mice were randomly divided into control group and CKD group, and CKD treated with lactoferrin (CKD+Lf) group for coadministration experiment to examine its preventative effect (Fig. 1A). In another experiment, mice were randomly divided into control group and CKD group, and CKD treated with lactoferrin (CKD+Post-Lf) group for post-administration experiment to examine its effect on already advanced CKD (Fig. 6A). At eight weeks of age, the control group was maintained under

normal diet, while CKD group and CKD+Lf group was fed a diet containing 0.2% adenine for six weeks. For coadministration experiment, the mice were supplied with tap water containing 2% lactoferrin (NRL Pharma Inc., Kanagawa, Japan) or control tap water ad libitum for the six weeks on the adenine diet. For postadministration experiment, the mice were supplied with 2% lactoferrin ad libitum for four consecutive weeks from week 7 after the 6-week adenine diet. The dosage of lactoferrin was set based on the dosage reported in previous studies [27]. At the end of this period, urine and blood samples were collected. The mice were anesthetized with isoflurane and then euthanized. Mouse organs were collected and quickly preserved in liquid N₂ or fixed in 2% paraformaldehyde for analysis. The body weight and organ weight at the dissection are summarized in Supplementary Table S1 and S2.

2.2. Quantitative real-time PCR analysis

TRI Reagent (Molecular Research Center Inc., Cincinnati, OH, USA) was used for RNA extraction according to the manufactures' protocol. For reverse transcription, Advanced cDNA Synthesis Kit for RT-qPCR (Bio-Rad Laboratories, Inc., Hercules, CA, USA) was used according to the manufacturer's protocol. For quantitative real time-PCR (qRT-PCR), primer of *Gapdh*, *Ctgf*, *Tgfb1*, and were purchased from Takara (Kusatsu, Japan), and primer of *Col1a1*, *Col3a1*, *Col4a1*, and *Pai1* were synthesized by Fasmac Co., Ltd (Kanagawa, Japan) and their set ID and sequence were listed in Supplementary Table S1. Gene expressions were evaluated using Luna® Universal qPCR Master Mix (NEW ENGLAND BioLabs, Massachusetts, USA) with Bio-Rad CFX real-time PCR system. As reference gene, *Gapdh* was used. The data were analyzed using the calibration curve method.

2.3. Renal histological analysis

The kidney was fixed with 2% paraformaldehyde, and paraffin embedding was performed by the Laboratory Animal Pathology Platform, Common Equipment Office, Tohoku University Graduate School of Medicine. Kidney sections were stained with Elastica Masson (EM) stain. EM-stained sections were used for renal tubular area evaluation, and sections were observed and photographed on a Keyence BZ-X800 (KEYENCE Corporation, Osaka, Japan).

2.4. Immunohistochemistry staining

We used rat anti mouse F4/80 monoclonal antibody (1:200, MCA497RT RRID: AB_1102558, Clone A3-1, BIO-RAD, Hercules, CA, USA) as primary antibody. Antigen retrieval was performed using Proteinase K (Agilent Technologies, CA, USA) incubated for 5 min at room temperature to detect F4/80. Primary antibodies were incubated overnight at 4°C. N-Histofine simple stain kit (Nichirei Biosciences, Tokyo, Japan) were used as a secondary antibody according to the manufacturer's protocol. Sections were incubated without primary antibody as a negative control. The ratio of the F4/80 positive area to tubulointerstitial area was assessed using Image J software.

2.5. Muscle histological analysis

Musculus quadriceps femoris were fixed with 2% paraformaldehyde, and paraffin embedding, H&E-staining was performed by the Laboratory Animal Pathology Platform, Common Equipment Office, Tohoku University Graduate School of Medicine. H&E-stained sec-

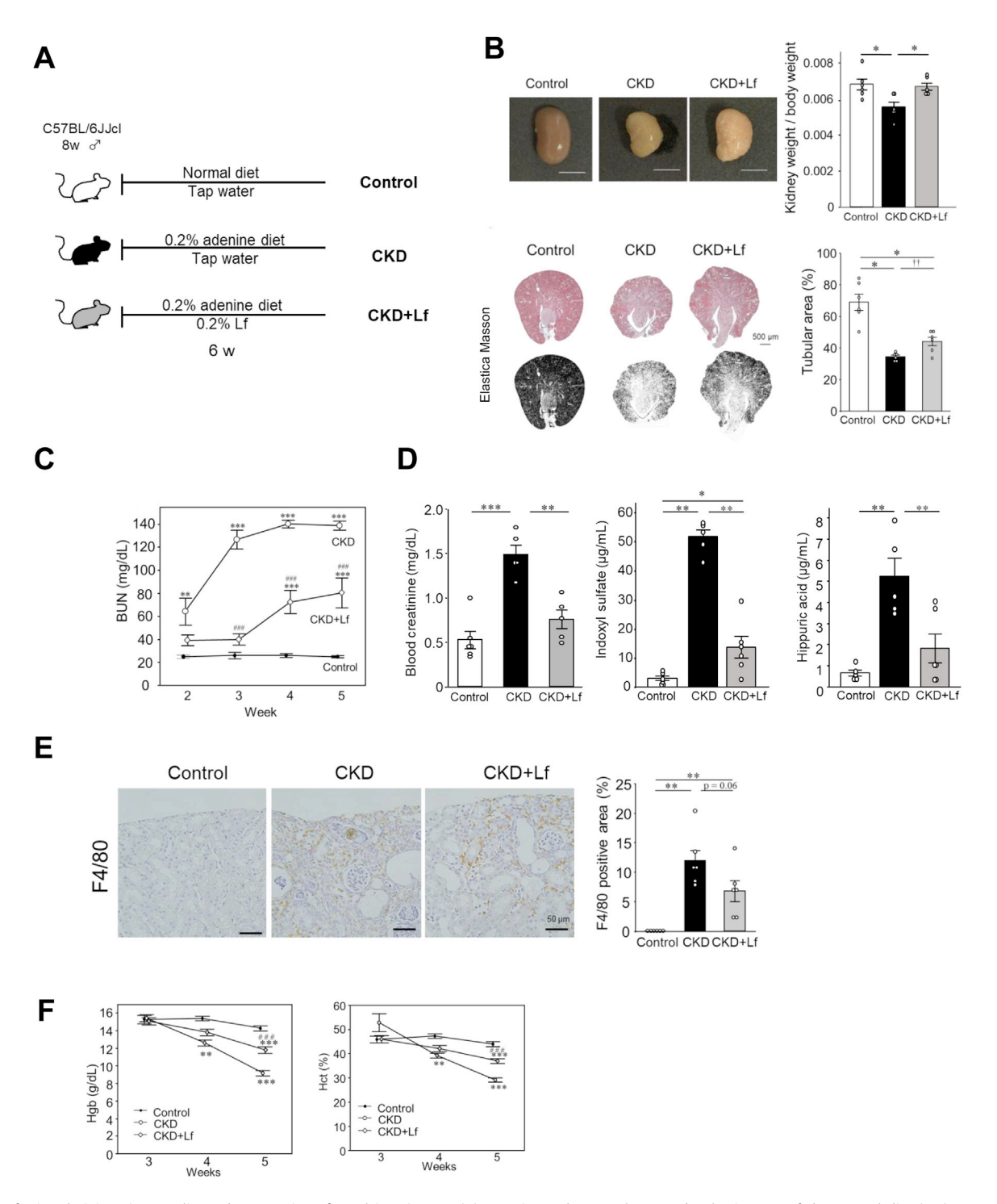


Fig. 1. Lactoferrin administration ameliorated progression of renal impairment. (A) Experimental protocols. C57BL/6JJcl mice were fed a normal diet (MF) or 0.2% adenine-containing diet. Lactoferrin (Lf) was dissolved in tap water. (B) Representative image of harvested kidney and kidney weight at 6 weeks after the start of the experiment. Representative images of Masson Trichrome staining and quantitative analysis of residual tubular are. (C) Concentrations of blood urea nitrogen (BUN) through 2 weeks to 5 weeks from start of experiment. (D) Levels of plasma creatinine, indoxyl sulfate, and hippuric acid. (E) Representative images of immunohistochemistry staining for F4/80 and quantitative analysis of F4/80 positive area, Tukey-Kramer's test; *P<.05, **P<.01, ***P<.01, ***P<.01

tions were used for muscle evaluation, and sections were observed on an OLYMPUS BX50 (Olympus Corporation, Tokyo, Japan) and photographed on a Leica FLEXACAM C1 (Leica Microsystems, Wetzlar, Germany). Thirty cross-sections of myofibers were randomly selected from each group for evaluation of cross-sectional area.

2.6. Gas chromatography-mass spectrometry measurements

The methods here reference our previous methods [27,28]. Fifty μg of quadriceps muscle was homogenized with 250 μL of a solution containing 55% methanol and 22% chloroform dis-

solved in distilled water containing 0.5 mg/mL 2-isopropylmalate (Sigma-Aldrich). Then, dissolved in distilled water was incubated in Thermo mixier C (Eppendorf) at 37°C with 1,200 rpm shaking for 30 min. The samples were centrifuged at 4° C and $16,000 \times g$ for 3 min. 225 µL of supernatant was collected and 200 µL of distilled water was added. The sample was dried using an evaporator under reduced pressure and lyophilized. For oximation, 80 µL of 20 mg/mL methoxyamine hydrochloride (Sigma-Aldrich) dissolved in pyridine were mixed with the lyophilized sample, sonicated for 20 min, and shaken at 1,200 rpm for 90 min at 30°C. Next, 40 μ L of N-methyl-N-trimethylsilyl-trifluoroacetamide (MSTFA) (GL Sciences, Tokyo, Japan) were added for derivatization. The mixture was then mixed at 1,200 rpm for 30 min at 37°C, centrifuged at $16,000 \times g$ for 5 min at 4°C, and the resulting supernatant (1 μ L) was subjected to GC-MS. GC-MS analysis was performed using a GC-MS QP2010 Ultra (Shimadzu) with a fused silica capillary column (BPX-5; 30 $m \times 0.25$ mm inner diameter, film thickness: 0.25 μ m; Shimadzu) and a front inlet temperature of 250°C, and a helium gas flow rate through the column of 39.0 cm/seconds. The column temperature was held at 60°C for 2 min, then raised by 15°C/min to 330°C and maintained for 3 min. The interface and ion source temperatures were 280°C and 200°C, respectively. All data obtained by GC-MS analysis. The retention times indicated in the Smart Metabolites Database (Shimadzu) were used. To perform a semi-quantitative assessment, the peak area of each quantified ion was calculated and normalized using 2-isopropylmalate peak area.

2.7. BUN measurement

Blood urea nitrogen (BUN) was measured using a BUN colorimetric detection kit (ARBOR ASSAYS, Ann Arbor, MI, USA) according to the manufacturer's instructions. Briefly, 50 μL of each plasma or standard reagent was added into wells, followed by 75 μL of Color Reagent A and 75 μL of Color Reagent B into each well. The plate was incubated at room temperature for 30 min, and the absorbance was recorded at 450 nm.

2.8. Uremic toxins measurement

These measurements reference to our previous reported methods [13,15]. For sample preparation, 150 μL of 0.1% formate methanol containing 2.0 μg/mL creatinine-d_{3.} 1.25 μg/mL indoxyl sulfate-d₃, and 2.5 μg/mL hippuric accid-d₅ were added to 50 μL of each plasma and vortexed for 1 sec. Then, the samples were sonicated for 5 min and centrifuged at $16,400 \times g$ for 20 min at 4°C. The supernatant was filtered through membranes. Quantitative analysis of indoxyl sulfate and hippuric acid was performed using LC-MS/MS using Nanospace SI-2 3,033 coupled to a TSQ Quantum Ultra mass spectrometer and operated in negative mode. For indoxyl sulfate and hippuric acid measurements, each sample (1 μ L) was injected into 100 \times 2.0 mm CAPCELL PAK C18 MG III, 3-µm column (OOSAKA SODA, Osaka, Japan) with Scherzo SM-C18 guard column 5 × 2.0 mm (Imtakt Corporation, Kyoto, Japan) at a flow rate of 0.2 mL/min. For gradient elution, mobile phase A was 10 mM ammonium acetate in pure water, and mobile phase B was acetonitrile. Linear and stepwise gradients were programmed as follows: 0-8 min: 0-100% solvent B; 8-12 min: 100% solvent B; 12-15 min: 0% solvent B. Quantification analysis by MS/MS was performed in SRM mode, wherein the transitions of the precursor ion to the product ion and collision energy were monitored: m/z212 \rightarrow 80, 21 V for indoxyl sulfate; m/z 216 \rightarrow 80, 30 V for indoxyl sulfate-d₄ m/z 178 \rightarrow 134, 13 V for hippuric acid; and m/z

 $183 \rightarrow 139$, 27 V for hippuric acid- $d_{5,}$. Spray voltage was 2,500 V, vaporizer temperature was 450°C, and capillary temperature was 220°C.

For creatinine measurement, each sample (1 μ L) was injected into 150 \times 2.0 mm YMC-PACK Pro C18, 3- μ m column (YMC Co., Ltd. Tokyo, Japan) with YMC semi-micro cartridge Pro C18 10 \times 2.0 mm (YMC Co., Ltd.) at a flow rate of 0.1 mL/min. The transitions of the precursor ion to the product ion and collision energy were monitored: m/z 114 \rightarrow 44, 17 V for creatinine; m/z 117 \rightarrow 47, 17 V for creatinine-d₃.

2.9. Western blotting

Protein was extracted using 1 × RIPA buffer (Cell Signaling Technology, Danvers, MA, USA) containing a protease inhibitor (Roche Diagnostics K.K, Tokyo, Japan), phosphatase inhibitor cocktail (Sigma Aldrich), and 1 mM PMSF (Thermo Scientific, Waltham, MA, USA). Protein concentration was determined using a Quick Start protein assay (Bio-Rad Laboratories, Hercules, CA, USA), and 25 μ g of protein was used in each SDS-PAGE run. TGX FastCast Acrylamide kit 12% Gel (Bio-Rad) was used for each analysis. Protein extracts were transferred to a PVDF membrane. After blocking for 1 h, the membrane was incubated with primary antibodies (anti-p70S6 Kinase, 1:1000, #9202, RRID: AB_331676, Cell Signaling; anti-Phospho p70S6 Kinase, 1:1000, #9205, RRID: AB_330944, Cell Signaling; anti-Phospho-4E-BP1, 1:1000, #9459 RRID:AB_330985, Cell Signaling, anti-TNF α , 1:1000, #250844 RRID:AB_2204102, ABBIOTEC; anti-MuRF-1, 1:1000, #MP3401 RRID: AB_2208832, ECM biosciences; anti-mTOR, 1:1000, #2972 RRID:AB_330978, Cell Signaling; anti-Phospho-mTOR, 1:1000, #2971 RRID:AB_330970, Cell Signaling; anti-AMPK α , 1:1000, #2532 RRID:AB_330331, Cell Signaling; anti-Phospho-AMPK, 1:1000, #2531 RRID:AB_330330, Cell Signaling; anti- LC3A/B, 1:2000, #12741 RRID:AB_2617131, Cell Signaling; anti-Cathepsin B, 1:1000, #31718 RRID:AB_2687580, Cell Signaling, anti- β -actin(C4), 1:1000, #sc-47778 RRID:AB_626632, Santa Cruz Biotechnology) overnight at 4°C. After washing, the membrane was incubated with secondary antibodies (anti-rabbit IgG, 1:5000, sc-2357 RRID:AB_628497, Santa Cruz Biotechnology, Dallas, TX, USA; anti-mouse IgG, 1:5000, sc-2031 RRID:AB_631737, Santa Cruz) for 1 h at room temperature. As a reference protein, β -actin was used.

2.10. Analysis of murine fecal microbiota

The measurement reference to our previous paper [29,30]. Feces were collected and stored at -30°C until DNA extraction. DNA was extracted from the mice fecal samples by the bead beating method using glass beads. The feces were placed in 2-mL vials (WAKENBTECH Co., Ltd., Tokyo, Japan) containing 0.5 mL of lysis buffer (No. 10, Kurabo Industries Ltd., Osaka, Japan) and 0.5 g of 0.1-mm glass beads. The mixture was mechanically disrupted by bead beating using a Cell destroyer PS1000 (Bio Medical Science, Tokyo, Japan) at 4,260 rpm for 50 s at room temperature. DNA was extracted from the homogenized sample using a Gene Prep Star PI-80X device (Kurabo Industries Ltd). The concentration of the extracted DNA was determined using a NanoDrop Spectrophotometer ND-1000 (Thermo Fisher Scientific Inc., Waltham, MA, USA), and samples were stored at -30° C until use. The V3-V4 region of the 16S rRNA gene was amplified from the fecal DNA samples by PCR using the following primers: forward: 5'-TCGTCGGCAGCGTCAGATGTGTATAAGCGACAGCCTACGGGNGGCWG CAG-3', and reverse: 5'-GTCTCGTGGGCTCGGAGATGTGTATAAGAGAC AGGACTACHVGGGTATCTAATCC-3'. DNA library for Illumina MiSeq

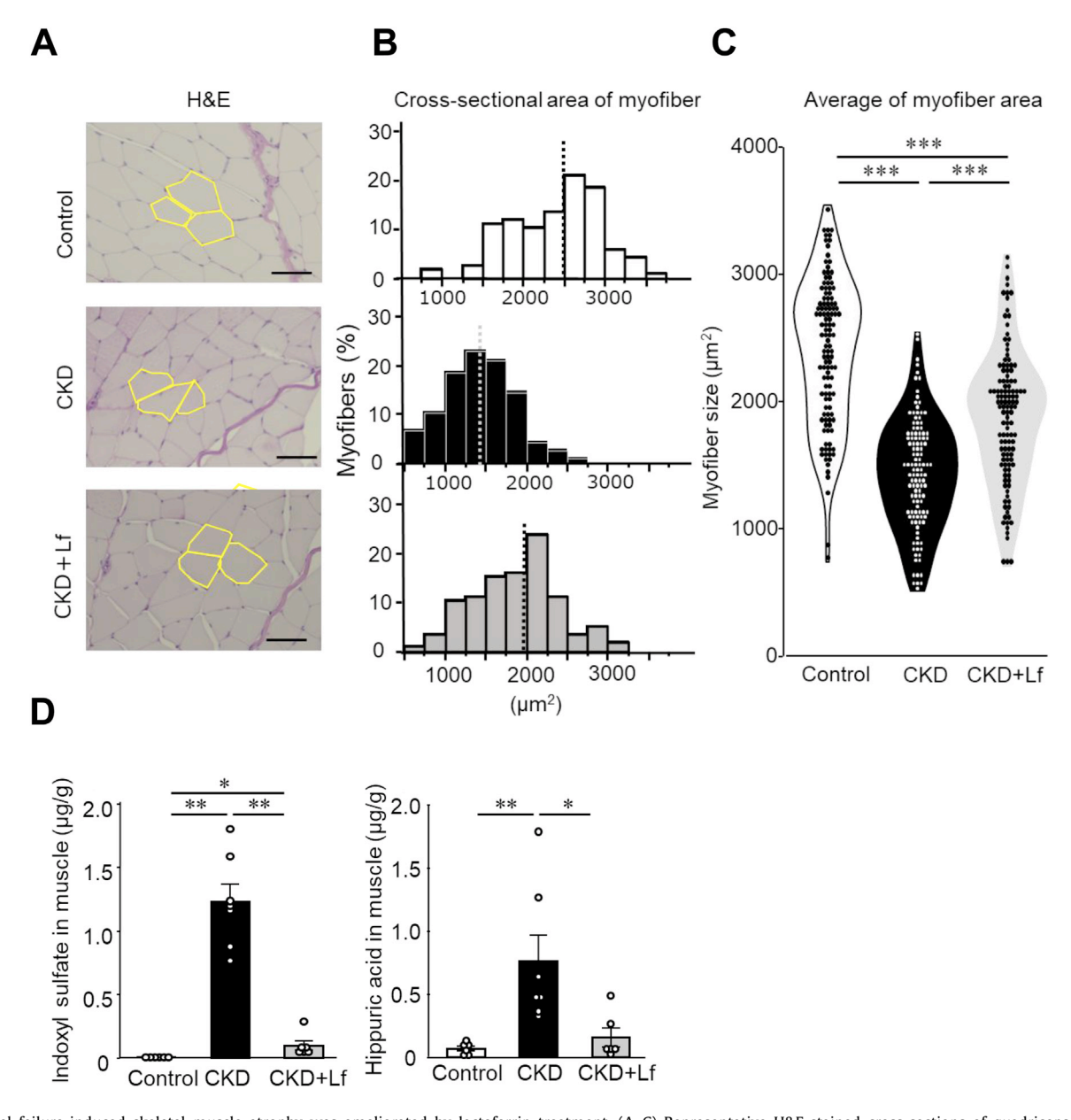


Fig. 2. Renal failure-induced skeletal muscle atrophy was ameliorated by lactoferrin treatment. (A–C) Representative H&E-stained cross-sections of quadriceps muscle. The yellow circular line is an example of a round-shaped muscle fiber used for the measurements. The number of evaluated cross-sectional area was 20 myofibers in each sample. (D) Levels of uremic toxins in quadriceps muscle. n=6 in each group. Data are shown as the mean \pm standard error of mean, Tukey-Kramer's test; *P<.01, ***P<.01, ***P<.001.

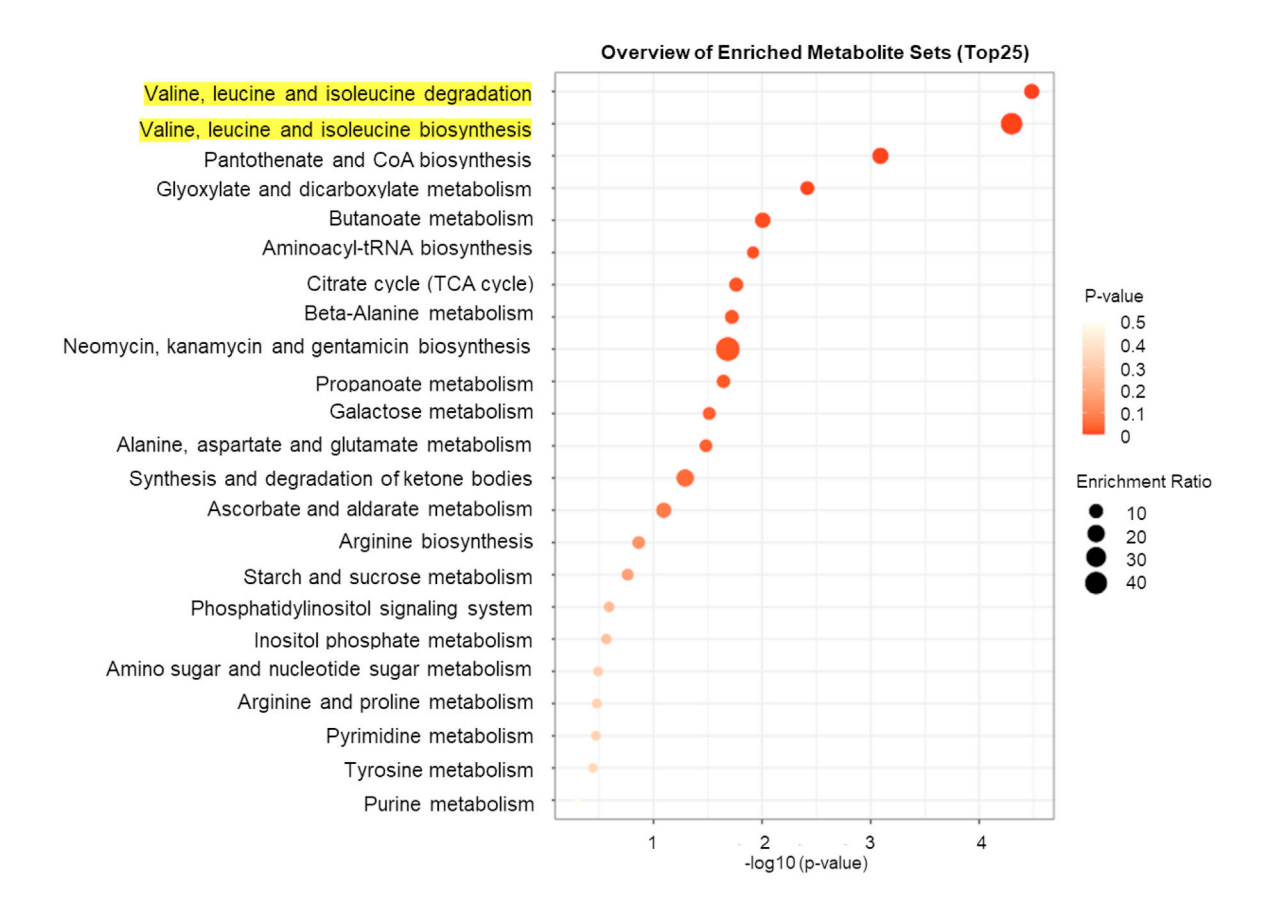
was prepared by using Nextera XT Index kit v2 set A (Illumina Inc., San Diego, CA, USA). 16S rRNA gene sequencing was performed using an Illumina MiSeq apparatus in accordance with the manufacturer's instructions. MiSeq reads were analyzed using the Quantitative Insights Into Microbial Ecology (QIIME) software package. The steps from trimming of pairedend reads to OTU picking were performed automatically by QIIME Analysis Automating Script (Auto-q) (Mohsen A, Park J, Kawashima H, Chen YA, Natsume-Kitatani Y, Mizuguchi K Auto-q Qiime Analysis Automating Script (version 1.0). Zenodo. 2018. http://doi.org/10.5281/zenodo.1439555.). OTU picking and taxonomic assignment were performed based on sequence similarity (>97%) using open-reference OTU picking with UCLUST software against the SILVA v128 reference sequence. Whole genome information of a specific microbe was obtained from SILVA browser and GenBank database.

2.11. Hematocrit and hemoglobin measurement

Hematocrit and hemoglobin levels were measured by automated animal hematology analyzers HORIBA Microsemi LC-662 (HORIBA, Ltd., Kyoto, Japan).

2.12. Statistical analysis

Data were analyzed using JMP software version 17.0.0 (SAS Institute Inc., Cary, NC, USA). Differences were considered statistically significant at P<.05. Student's t-test was used for two variables comparisons. Statistical comparisons of multiple groups were made using analysis of variance, followed by the Tukey-Kramer test for normal distribution. In the case of non-normal distribution, Wilcoxon test, followed by the Steel-Dwass test was used. Values



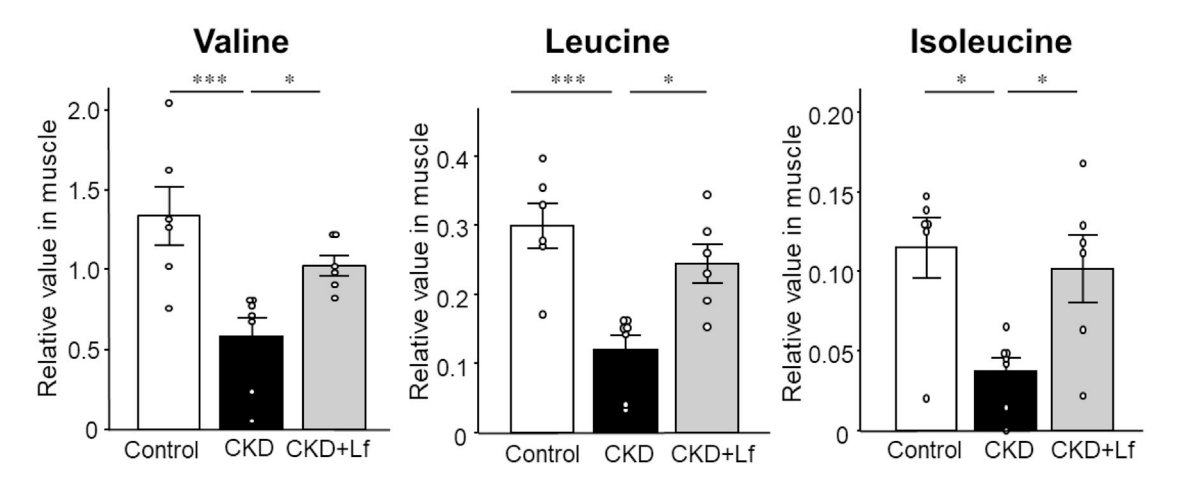


Fig. 3. Changes in valine, leucine and isoleucine metabolism in the skeletal muscle. Enrichment analysis of metabolite sets in the skeletal muscle between control group and chronic kidney disease (CKD) group. Levels of valine, leucine, and isoleucine in the skeletal muscle of Control, CKD, and CKD+lactoferrin (Lf) group. The sample number of Control, CKD, and CKD+Lf group was n=6, n=7, n=6 in each group. Data are shown as the mean \pm standard error of mean, Tukey-Kramer's test; *P<.05, **P<.01, ***P<.001.

were presented as mean \pm standard error of the mean. The post hoc power analysis was performed using JMP software, with a significant level (α) set to 0.05, σ was the root mean square error, and effect size (δ) set to 0.5.

3. Results

3.1. Prophylactic lactoferrin supplementation attenuates the progression of kidney disease

To evaluate the impact of lactoferrin supplementation on the progression of CKD, mice were divided into three groups; control

group fed a normal diet, CKD group fed an adenine-containing diet, and CKD+lactoferrine (Lf) group fed an adenine containing diet along with 2% lactoferrin solution for six weeks (Fig. 1A). During the study period, CKD mice showed body weight loss, whereas the CKD+Lf group showed reduction in body weight loss (Supplementary Fig. 1A). Both CKD and CKD+Lf groups exhibited increased water consumption compared to the control group, with the CKD group consuming significantly more water than the CKD+Lf group from the 4 weeks of the study (Supplementary Fig. 1B). In the CKD group, the kidney weight was reduced along with a decrease in tubular area (Fig. 1B), whereas these reductions were mitigated by lactoferrin supplementation in the CKD+Lf group (Fig. 1B). Al-

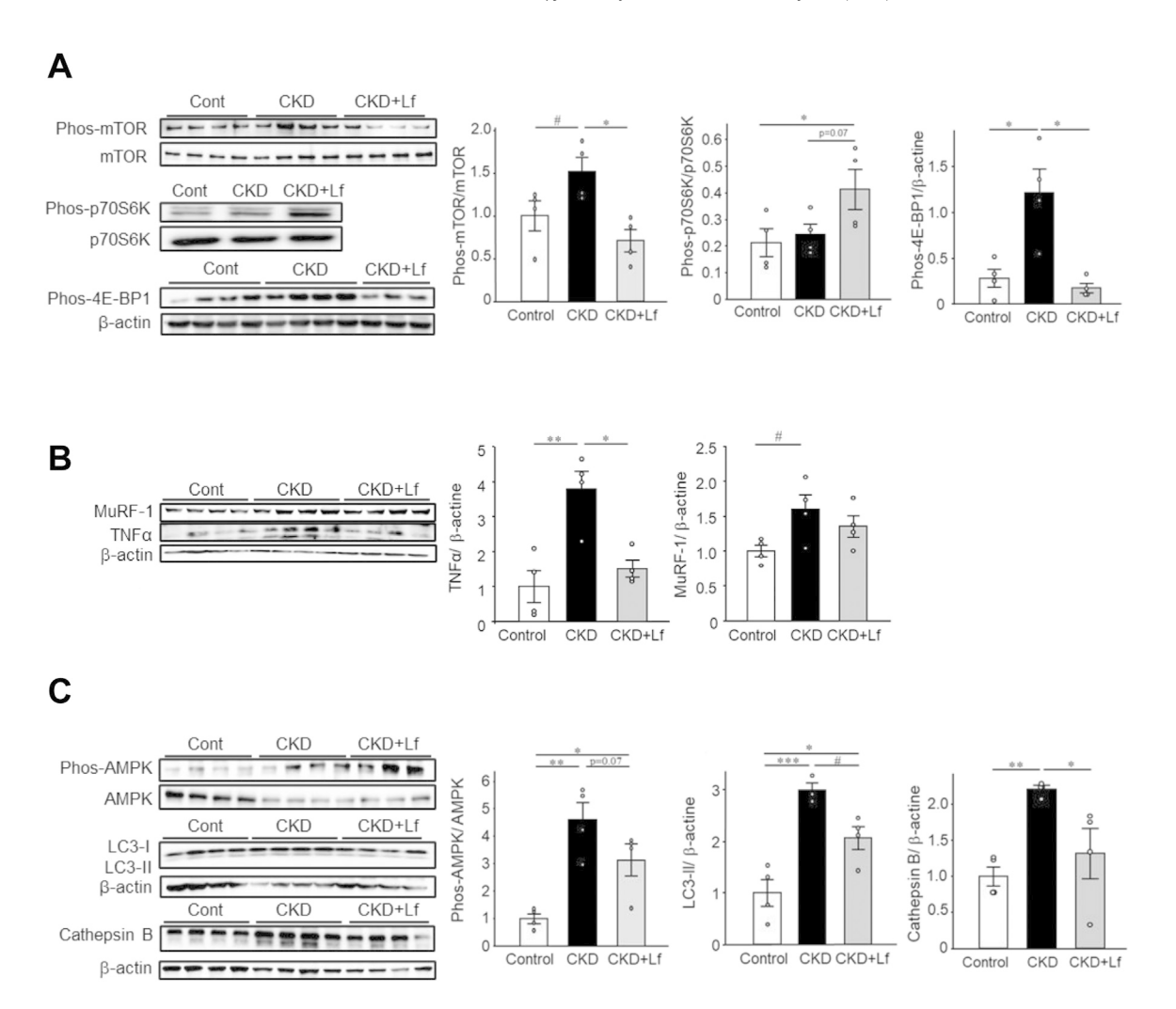


Fig. 4. Renal failure-induced autophagy in skeletal muscle was ameliorated by lactoferrin treatment. (A) Phosphorylation levels of mTOR, p70S6kinase (p70S6K), and 4E-BP1 in main anabolic signaling pathway. (B) The levels of TNFα and MuRF-1 in the catabolic pathway. (C) Phosphorylation of AMPK and levels of LC3-II and cathepsin B in autophagy-mediated protein degradation. The sample number of Control, CKD, and CKD+lactoferrin (Lf) group was n=4 each group. Data are shown as the mean \pm standard error of mean, Tukey-Kramer's test; *P<.05, **P<.01, ***P<.00.1. Student's t-test, *P<.05.

though markers of kidney function, including BUNplasma creatinine, and plasma uremic toxins (indoxyl sulfate and hippuric acid) were significantly elevated in the CKD group, these parameters were attenuated with lactoferrin supplementations (Fig. 1C and D). Furthermore, increased macrophage infiltration, shown by immunohistochemistry stained with F4/80, observed in the kidney of the CKD group was notably reduced in the CKD+Lf group (P=.06) (Fig. 1E).

In addition, lactoferrin administration alleviated renal anemia, as evidenced by improved hemoglobin and hematocrit levels and red blood cell (RBC) concentrations, which were decreased in the CKD group (Fig. 1F, Supplementary Fig. 3). These findings indicate that lactoferrin supplementation attenuates fibrosis progression, and inflammation in the adenine-induced CKD model, thereby preventing the disease progression of CKD.

3.2. Effect of prophylactic lactoferrin supplementation on uremic sarcopenia

We previously reported that uremic toxins, such as indoxyl sulfate, accumulate in skeletal muscle and is involved in development of uremic sarcopenia via metabolic alteration [13,15]. To assess the effect of lactoferrin in uremic muscle atrophy, we analyzed

the morphological structure of the quadriceps muscle (Fig. 2A–C). The cross-sectional area of skeletal muscle fiber was significantly smaller in CKD group compared to control group. However, lactoferrin supplementation ameliorated the skeletal muscle atrophy observed in CKD group. In addition, we found that the levels of uremic toxins, such as indoxyl sulfate and hippuric acid, were higher in the skeletal muscle of CKD group mice than in the control group, and these levels were significantly reduced in the CKD+Lf group (Fig. 2D).

To investigate the effects of lactoferrin on metabolic pathways in CKD, metabolomic analysis of the quadriceps muscle was conducted. Enrichment analysis highlighted alterations in the degradation and biosynthesis pathways of valine, leucine, and isoleucine, indicating decreased levels of these branched-chain amino acids (BCAAs) in the skeletal muscle of the CKD group (Fig. 3). Since BCAAs are known to be involved in protein synthesis pathways and proteolytic pathways, specifically the ubiquitin-proteasome system (UPS) and the autophagy-lysosome system, we examined the involvement of each pathway in the progression of sarcopenia and the effect of lactoferrin. BCAA enhance the phosphorylation status of key proteins with mammalian target of rapamycin (mTOR) signaling pathway, whose activation is a marker for muscle protein synthesis [31,32]. In the mTOR pathway, the phosphorylation level of mTOR, p70S6K and 4E-BP1 indicate the activation of mTOR

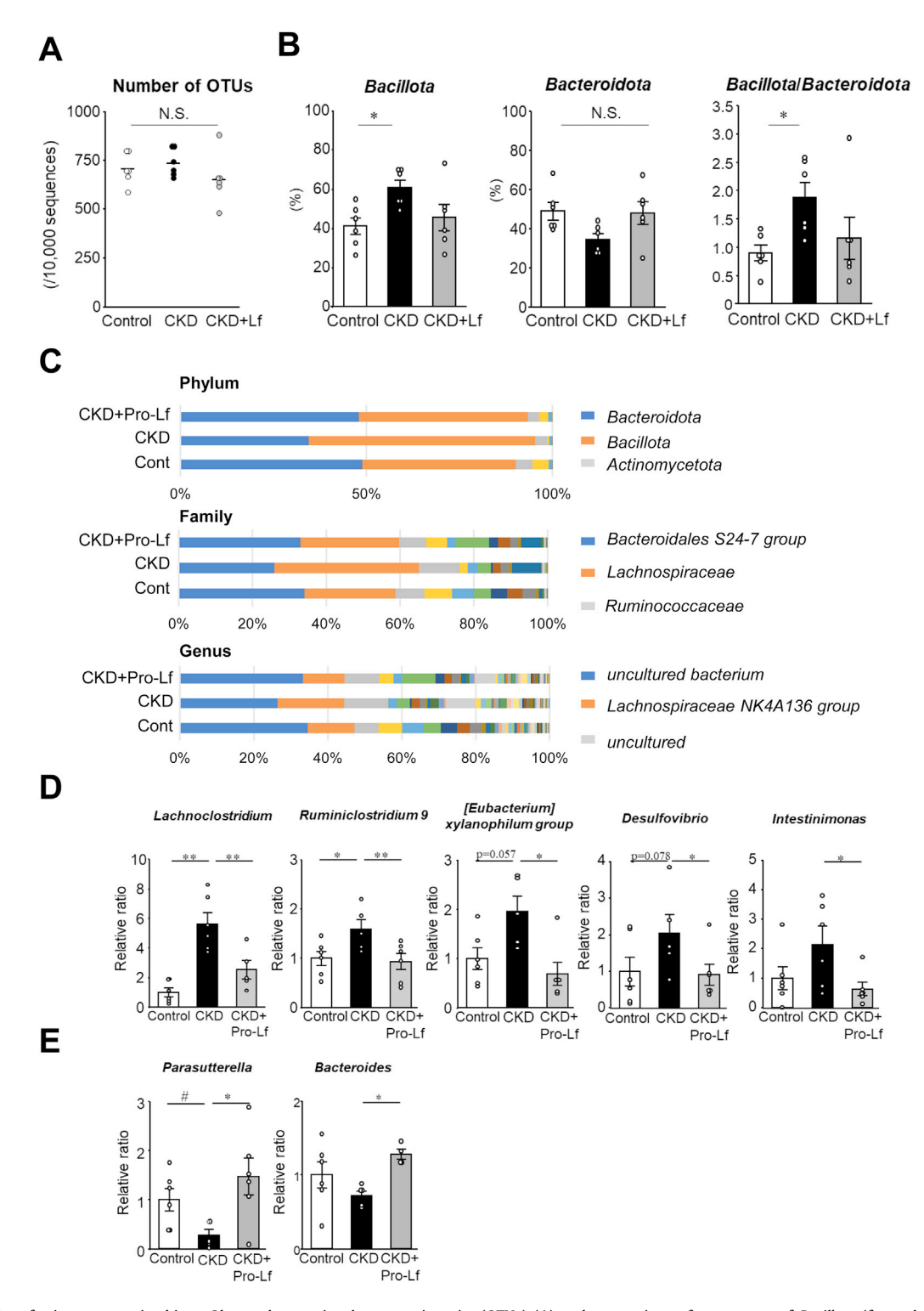


Fig. 5. Effect of lactoferrin on gut microbiota. Observed operational taxonomic units (OTUs) (A) and comparison of percentage of *Bacillota* (formerly *Firmicutes*) and *Bacteroidota* (formerly *Bacteroidotes*) (B). (C) Relative abundance of microbiota based on the average number of each subfamily at the phylum, family, and genus levels. The major subfamilies are indicated next to the figure. (D-E) Relative abundances of *Lachnoclostridium*, *Ruminiclostridium* 9, [Eubacterium] xylanophilum group, Desulfovibrio, Intestinimonas, Parasutterella, and Bacteroides. Data are shown as the mean \pm standard error of mean, Tukey-Kramer's test; *P<.0.5, **P<.01, n=6 per group. Student's t-test, *P<.05.

signaling [33,34]. In the CKD group, the phosphorylation levels of mTOR and 4E-BP1 were increased compared to the control group. Although the phosphorylation level of p70S6K did not differ between the control and CKD groups, it was significantly higher in the CKD+Lf group than in the control group (Fig. 4A). Among the catabolic pathway of skeletal muscle, a E3 ubiquitin ligase mus-

cle RING finger (MuRF1) and tumor necrosis factor-alpha (TNF- α) are associated with loss of skeletal muscle strength [35]. The expression levels of TNF- α and MuRF1 in the quadriceps muscle were increased in the CKD group compared to those of the control group (Fig. 4B). CKD-induced mTOR and 4E-BP1 phosphorylation indicate suppression of autophagy pathway, however, 5′-

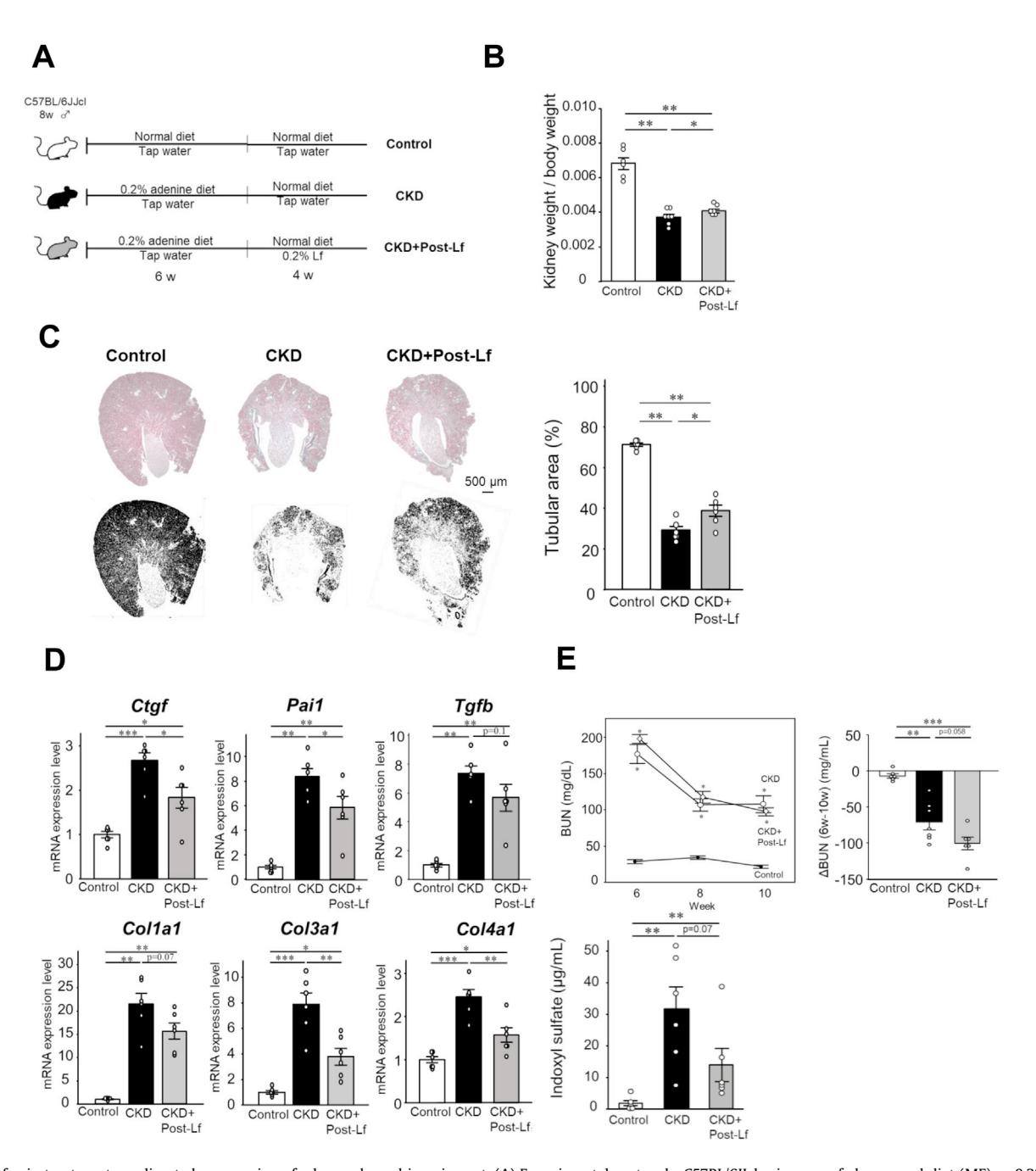


Fig. 6. Lactoferrin treatment ameliorated progression of advanced renal impairment. (A) Experimental protocols. C57BL/6JJcl mice were fed a normal diet (MF) or 0.2% adenine-containing diet. Lactoferrin (Lf) was dissolved in tap water. (B) Comparisons of weight of the kidney and the heart. (C) Representative images of Masson Trichrome staining and quantitative analysis of residual tubular area. (D) Gene expression levels of *Ctgf, Pai1, Tgfb, Col1a1, Col3a1*, and *Col4a1* in the kidney. (E) Concentrations of blood urea nitrogen (BUN) through 6 weeks to 10 weeks to 10 weeks from start of experiment and the change in BUN from 6 weeks to 10 weeks (△BUN). Comparison of plasma concentration of indoxyl sulfate. Data are shown as the mean ± standard error of mean, Tukey-Kramer's test; ****P<.001 **P<.05, ***P<.01, ****P<.001, n=6 per group.

adenosine monophosphate-activated protein kinase (AMPK), which acts as a key regulator of skeletal muscle metabolism with promoting autophagy-mediated protein degradation [36], was significantly increased in the CKD group. The phosphorylation level of AMPK was significantly increased in CKD group compared to the control group (Fig. 4C). Conversion of LC3-I to LC3-II, a marker of autophagosome formation [37] and the expression of cathepsin B, a lysosomal cysteine protease crucial for intracellular protein in lysosomes [38] were significantly increased in CKD group compared to the control group. This increase was ameliorated by lactoferrin administration (Fig. 4C). Taken together, despite decreased BCAA levels with altered BCAA metabolism in skeletal muscle of the CKD

group, the mTOR, UPS and autophagy system were irregularly promoted under the CKD condition. This abnormal activation of these proteolysis pathways in CKD was ameliorated by lactoferrin administration. These results suggest that lactoferrin administration attenuates uremic sarcopenia.

3.3. Effect of prophylactic lactoferrin supplementation on gut microbiota

Since lactoferrin administration decreased plasma level of microbiota-derived uremic toxins, such as indoxyl sulfate, in the CKD mice (Fig. 1C), we examined the impact of lactoferrin sup-

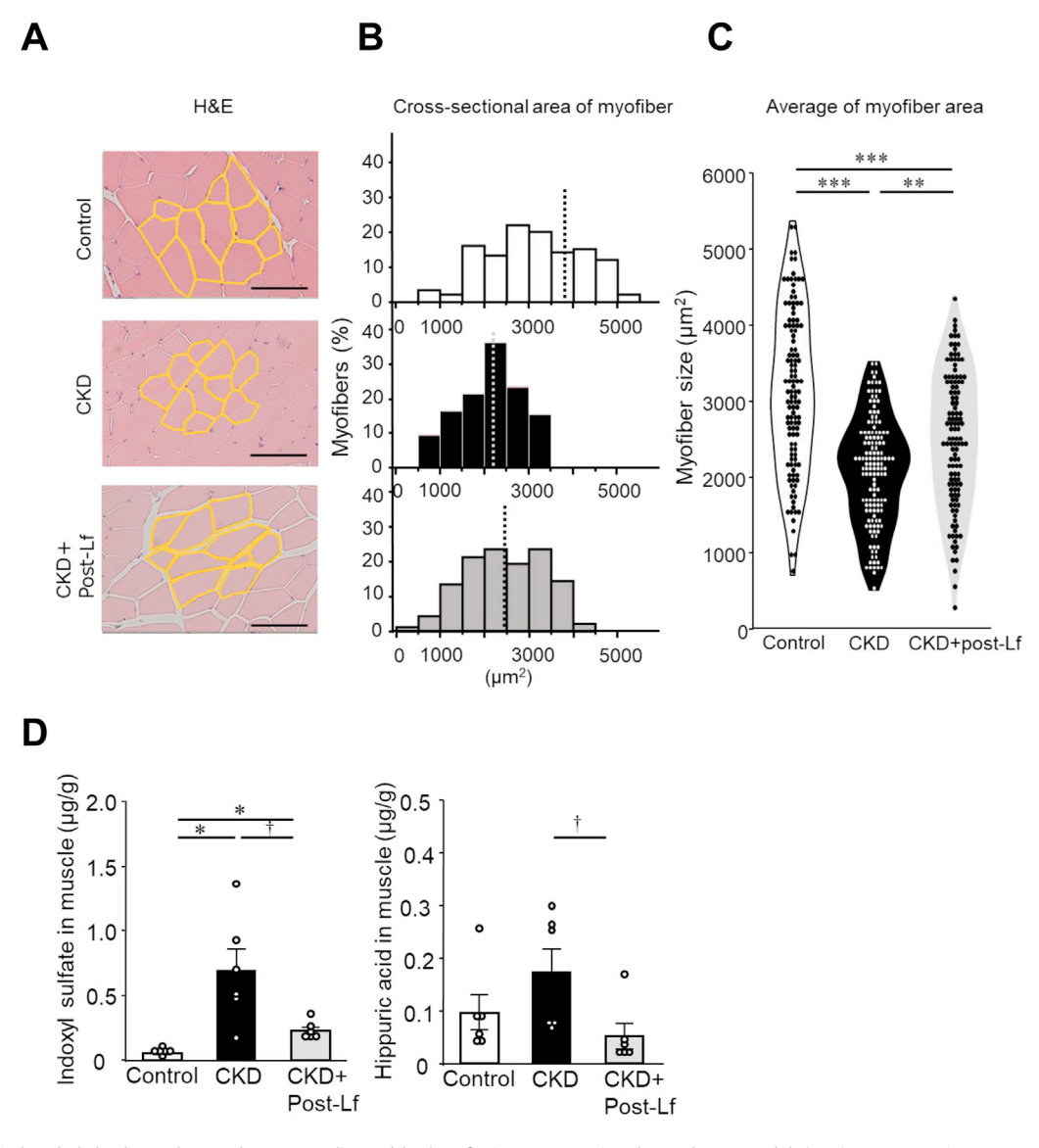


Fig. 7. Renal failure-induced skeletal muscle atrophy was ameliorated by lactoferrin treatment in advanced CKD model. (A–C) Representative H&E-stained cross-sections of quadriceps muscle. The yellow circular line is an example of a round-shaped muscle fiber used for measurements. The number of evaluated cross-sectional area was 30 myofibers in each sample. (D) Levels of uremic toxins in quadriceps muscle. n=6 in each group. Data are shown as the mean \pm standard error of mean, Tukey-Kramer's test; *P<.05, **P<.05, *P<.05, **P<.05, **P<.05, **P<.05, **P<.05, **P<.05, *P<.05, **P<.05, **P<.05, **P<.05, **P<.05, **P<.05,

plementation on gut microbiota composition in CKD condition. The number of identified operational taxonomic units (OTUs) did not differ among the three groups (Fig. 5A). At the phylum level, Bacillota (formerly Firmicutes) were significantly increased in the CKD group compared to the control group, while Bacteroidota (formerly Bacteroidetes) remained consistent across three groups (Fig. 5B and 5C). The Bacillota/Bacteroidota ratio, an indicator of microbiota composition changes [39]. Bacillota/Bacteroidota ratio was significantly increased in the CKD group compared to the control group. At the family and genus level, minor populations of gut microbiota varied among the groups (Fig. 5C). Specifically, seven species showed significant changes by CKD condition or lactoferrin supplementation (Fig. 5D and E). The relative abundance of Lachnoclostridium, Ruminiclostridium 9, [Eubacterium] xylanophilum group, Desulfovibrio, and Intestinimonas increased in the CKD group compared to the control group (Fig. 5D). Conversely, Parasutterella and Bacteroides decreased in the CKD group (Fig. 5E). Lactoferrin administration ameliorated these CKD-related dysbiosis.

3.4. Effect of lactoferrin supplementation on advanced renal impairment

In addition to the preventive effect, we examined the effect of lactoferrin on already advanced renal damage. For this purpose, mice were fed an adenine-containing diet for 6 weeks, followed by 4 weeks of lactoferrin supplementation (Fig. 6A). Both CKD and lactoferrin-supplemented CKD mice (CKD+Post-Lf group) showed weight gain after returning to a normal diet, with no significant differences observed between the two groups (Supplementary Fig. 2A). While the kidney weight was reduced in CKD mice, lactoferrin administration ameliorated this kidney reduction (Fig. 6B). The tubular area in the kidney was also better preserved in the CKD+Post-Lf group compared to the CKD group (Fig. 6C). Regarding inflammation and fibrosis in the damaged kidney, increased expression levels of inflammatory cytokine and pro-fibrotic genes, such as Ctgf, Pai1, Tgfb, Col1a1, Col3a1, and Col4a1, in the CKD group were mitigated by lactoferrin administration (Fig. 6D). Kidney function parameter, such BUN showed no significant differences between CKD and CKD+-Post-Lf at dissection. However, the change in BUN from 6 weeks to 10 weeks (\triangle BUN) was greater in the CKD+Post-Lf group than in the CKD group. In addition, plasma level of indoxyl sulfate was reduced in the CKD+Post-Lf group (Fig. 6E). Taken together, these findings suggest that lactoferrin treatment attenuated kidney fibrosis and inflammation, even in the context of advanced renal damage.

3.5. Lactoferrin supplementation reduced uremic toxin accumulation and ameliorated muscle atrophy in advanced kidney disease

Finally, we evaluated the effects of post-administration of lactoferrin on muscle atrophy in advanced kidney disease by analyzing the morphological structure of the quadriceps muscle (Fig. 7A-C). The cross-sectional area of skeletal muscle was significantly smaller both in the CKD and the CKD+Post-Lf group compared to the control group. However, atrophied skeletal muscle, as evaluated by cross-sectional area, was ameliorated by lactoferrin postsupplementation in advanced kidney disease status. In addition, the levels of uremic toxins in skeletal muscle were reduced in the CKD+Post-Lf group (Fig. 7D). Metabolomic analysis of the quadriceps muscle was conducted to examine the effect of lactoferrin on muscle atrophy in advanced kidney disease. Enrichment analysis highlighted alterations in the biosynthesis pathways of valine, leucine, and isoleucine, indicating that lactoferrin affects levels of BCAAs in the skeletal muscle of the CKD group (Supplementary Fig. 4).

4. Discussion

In the present study, we investigated the effects of lactoferrin administration on the progression of CKD and the associated uremic sarcopenia, yielding several important findings. First, lactoferrin administration prevents the progression of renal damage by attenuating renal fibrosis and inflammation. Second, lactoferrin ameliorated CKD-associated uremic sarcopenia with modulating BCAA metabolism and abnormal autophagy signaling. Third, lactoferrin reduced the production of microbiota-derived uremic toxins by ameliorating dysbiosis, leading to decreased accumulation of uremic toxins in blood and muscle, which contributed to the suppression of renal damage and sarcopenia progression. Our study indicates the beneficial effects of lactoferrin and provides its mechanistic insight into its role in CKD progression and the associated uremic sarcopenia.

In addition to its renoprotective effect, lactoferrin ameliorated muscle atrophy and reduced accumulation of uremic toxins in muscle in CKD mice. Muscle fiber atrophy is well-recognized in patients with sarcopenia. Previous reports suggest that uremic toxins accumulate in the muscles of CKD mice, with indoxyl sulfate contributing to sarcopenia pathogenesis through inflammation, oxidative stress, and metabolic alterations [14,15]. Our results suggest that lactoferrin may inhibit uremic sarcopenia progression by modulating malnutrition and dysbiosis in CKD. The gut microbiota plays a crucial role in regulating the immune system and maintaining homeostasis. Recent evidence has highlighted that dysbiosis is a significant factor in the pathophysiology of CKD [19]. In addition to CKD, effects of lactoferrin on correcting dysbiosis have been reported in cognitive dysfunction [40], obesity [41,42], and inflammatory bowel disease [43]. In this study, lactoferrin partially improved dysbiosis in CKD (Fig. 5B). Correction of dysbiosis reduces accumulation of uremic toxins and CKD-related pathologies [44–46]. Therefore, our study suggests that lactoferrin's inhibitory effect on CKD and uremic sarcopenia progression may involve its potential to modulate the microbiota composition and inhibit uremic toxin production. Of note, previous animal studies showed

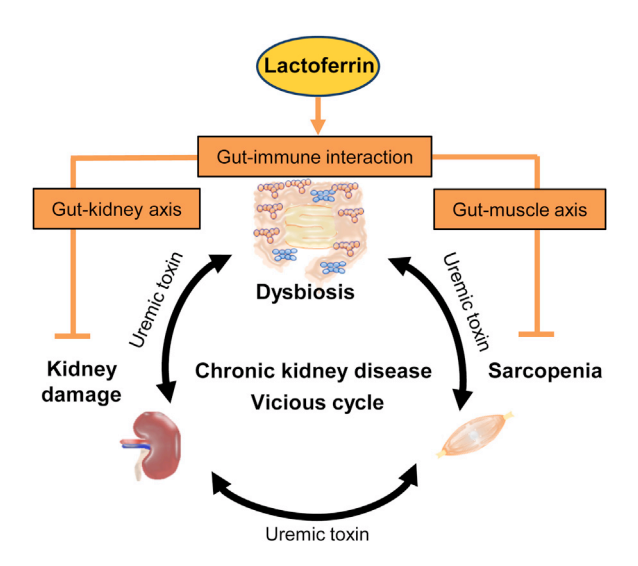


Fig. 8. Diagrams depicting the impact of lactoferrin on renal failure and uremic sarcopenia. Lactoferrin attenuates the vicious cycle that occurs during renal failure via the gut-kidney-skeletal muscle axis inhibiting the inflammation and fibrosis signaling in the kidney, suppressing the production of uremic toxins derived from intestinal microbiota, and correcting metabolic disturbances in skeletal muscle.

that lactoferrin is not detected in serum after oral administration, suggesting that its effects are primarily mediated through interactions within the intestinal tract, with hydrolysis products being absorbed through the gastrointestinal system [47]. Therefore, it is assumed that lactoferrin exerts its beneficial effects on the kidneys and muscles by acting on the intestines and gut microbiota.

Patients with CKD exhibit abnormal nutritional metabolism, including disruptions in BCAA metabolism, which lead to decreased intracellular BCAA concentrations [48]. BCAAs are degraded in skeletal muscle, and this degradation is associated with reduced intracellular BCAA concentrations. Previous studies have shown that increased BCAA degradation in skeletal muscle suppresses protein synthesis via mTORC1, leading to muscle atrophy, and that BCAA supplementation can suppress muscle atrophy [49]. In this study, CKD mice exhibited significant alterations in BCAA degradation and synthesis pathways, and lactoferrin administration ameliorated the reduction in BCAAs in the CKD group.

Although mTORC1 activation is known to correlate with increased muscle protein synthesis [33], CKD mice unexpectedly showed increased mTOR phosphorylation in the CKD group, which decreased with lactoferrin administration (Fig. 4A). Recent studies indicate that abnormally sustained activation of mTORC1 signaling may recapitulate features of sarcopenia [50]. Therefore, the sustained activation of mTORC1 observed in the skeletal muscle of CKD mice might contribute to muscle atrophy, and this activation appears to be suppressed by lactoferrin. Previous reports have demonstrated that AMPK signaling and autophagy are enhanced in the muscles of CKD mice [51,52]. Our findings suggest that the suppression of protein degradation via autophagy may also play a role in preventing the progression of CKD-related sarcopenia, and that lactoferrin further attenuated this process (Fig. 4C). In addition, the enhancement of autophagy induced by CKD needs to be confirmed by an autophagy-flux assay, but it is difficult to verify in vivo, which is the limitation of this study.

While no serious adverse events clearly associated with lactoferrin have been reported in healthy individuals following highdose administration, its administration to patients with kidney disease has not been investigated, so dosage should be carefully considered. Ingested lactoferrin is digested by pepsin and trypsin in the stomach and intestine, respectively, into lactoferricin peptide, which exhibits antioxidant, immunomodulatory effects [16,53–56]. Given that, lactoferrin was not detectable in the blood in the present study, its direct action to the kidneys or skeletal muscles is unlikely. Therefore, the protective effects of lactoferrin on the kidneys and muscles are probably considered to be mediated indirectly via gut-immune interactions, consistent with the gut-kidney and gut-muscle axis hypotheses. This study demonstrated that lactoferrin exhibits effects equivalent to those of nicotinamide, a vitamin B3 previously reported by our group [27]. The effect of lactoferrin against renal impairment differed from that of nicotinamide. Therefore, combining nutrients with different mechanisms of effect may yield synergistic or additive effects against renal impairment, and we plan to conduct further studies in the future.

In conclusion, lactoferrin attenuates the vicious cycle of CKD inhibiting inflammation and fibrosis signaling in the kidney, suppressing uremic toxin production derived from gut microbiota, and correcting metabolic disturbances in skeletal muscle, via the gut-kidney-skeletal muscle axis (Fig. 8).

Funding

This study was supported by JSPS KAKENHI Grant Number 19K08669 (E.S) and 23H03301 (E.S), 23K27991 (E.S) and The Koyanagi Foundation, and The Research Foundation for the Treatment of Metabolic Disorder.

Declaration of competing interests

The authors declare the following financial interests/personal relationships which may be considered as potential competing interests: Emiko Sato reports drug was provided by NRL Pharma Inc. Emiko Sato has patent #PCT/JP2024/017376 pending to Tohoku University. E.S and Y.I. have a patent application related to this work. If there are other authors, they declare that they have no known competing financial interests or personal relationships that could have appeared to influence the work reported in this paper.

CRediT authorship contribution statement

Yukina Iwamoto: Writing – original draft, Visualization, Methodology, Investigation. Seiko Yamakoshi: Writing – review & editing, Investigation, Formal analysis, Data curation, Conceptualization. Akiyo Sekimoto: Writing – review & editing, Investigation, Formal analysis, Data curation. Koji Hosomi: Writing – review & editing, Investigation, Formal analysis, Data curation. Takashi Toyama: Writing – review & editing, Formal analysis, Data curation. Yoshiro Saito: Writing – review & editing. Jun Kunisawa: Writing – review & editing. Nobuyuki Takahashi: Writing – review & editing, Supervision. Emiko Sato: Writing – review & editing, Supervision, Resources, Project administration, Methodology, Investigation, Funding acquisition, Formal analysis, Data curation, Conceptualization.

Acknowledgments

We acknowledge technical assistance from staff at the Division of Clinical Pharmacology and Therapeutics, Tohoku University Graduate School of Pharmaceutical Sciences. The authors thank NRL Pharm Inc. for kindly providing lactoferrin. We thank Laboratory Animal Pathology Platform, Common Equipment Office, Tohoku University Graduate School of Medicine for the support to the present study. We appreciate TUMUG of Tohoku University center for gender equality promotion.

Supplementary materials

Supplementary material associated with this article can be found, in the online version, at doi:10.1016/j.jnutbio.2025.110039.

References

- Foley RN, Wang C, Ishani A, Collins AJ, Murray AM. Kidney function and sarcopenia in the United States general population: NHANES III. Am J Nephrol 2007;27:279–86.
- [2] Giglio J, Kamimura MA, Lamarca F, Rodrigues J, Santin F, Avesani CM. Association of sarcopenia with nutritional parameters, quality of life, hospitalization, and mortality rates of elderly patients on hemodialysis. J Ren Nutr 2018;28:197–207.
- [3] Sabatino A, Regolisti G, Delsante M, Di Motta T, Cantarelli C, Pioli S, et al. Noninvasive evaluation of muscle mass by ultrasonography of quadriceps femoris muscle in End-Stage Renal Disease patients on hemodialysis. Clin Nutr 2019;38:1232–9.
- [4] Pereira RA, Cordeiro AC, Avesani CM, Carrero JJ, Lindholm B, Amparo FC, et al. Sarcopenia in chronic kidney disease on conservative therapy: prevalence and association with mortality. Nephrol Dial Transplant 2015;30:1718–25.
- [5] Johansen KL, Dalrymple LS, Delgado C, Chertow GM, Segal MR, Chiang J, et al. Factors associated with frailty and its trajectory among patients on hemodialysis. Clin J Am Soc Nephrol 2017;12:1100–8.
- [6] Lee SY, Yang DH, Hwang E, Kang SH, Park SH, Kim TW, et al. The prevalence, association, and clinical outcomes of frailty in maintenance dialysis patients. J Ren Nutr 2017;27:106–12.
- [7] Klinkhammer BM, Djudjaj S, Kunter U, Palsson R, VO Edvardsson, Wiech T, et al. Cellular and molecular mechanisms of kidney injury in 2,8-dihydrox-yadenine nephropathy. J Am Soc Nephrol 2020;31:799–816.
- [8] Lin YL, Liou HH, Wang CH, Lai YH, Kuo CH, Chen SY, et al. Impact of sar-copenia and its diagnostic criteria on hospitalization and mortality in chronic hemodialysis patients: a 3-year longitudinal study. J Formosan Med Associat = Taiwan yi zhi 2020;119:1219-29.
- [9] Durozard D, Pimmel P, Baretto S, Caillette A, Labeeuw M, Baverel G, et al. 31P NMR spectroscopy investigation of muscle metabolism in hemodialysis patients. Kidney Int 1993;43:885–92.
- [10] Mijnarends DM, Luiking YC, Halfens RJG, Evers S, Lenaerts ELA, Verlaan S, et al. Muscle, health and costs: a glance at their relationship. The journal of nutrition. Health & Aging 2018;22: 766–773.
- [11] Rao M, Li L, Demello C, Guo D, Jaber BL, Pereira BJ, et al. Mitochondrial DNA injury and mortality in hemodialysis patients. J Am Soc Nephrol 2009;20:189–96.
- [12] Tirichen H, Yaigoub H, Xu W, Wu C, Li R, Li Y. Mitochondrial reactive oxygen species and their contribution in chronic kidney disease progression through oxidative stress. Front Physiol 2021;12:627837.
- [13] Sato E, Saigusa D, Mishima E, Uchida T, Miura D, Morikawa-Ichinose T, et al. Impact of the oral adsorbent AST-120 on organ-specific accumulation of uremic toxins: LC-MS/MS and MS imaging techniques. Toxins (Basel) 2017;10:19.
- [14] Enoki Y, Watanabe H, Arake R, Sugimoto R, Imafuku T, Tominaga Y, et al. Indoxyl sulfate potentiates skeletal muscle atrophy by inducing the oxidative stress-mediated expression of myostatin and atrogin-1. Sci Rep 2016;6:32084.
- [15] Sato E, Mori T, Mishima E, Suzuki A, Sugawara S, Kurasawa N, et al. Metabolic alterations by indoxyl sulfate in skeletal muscle induce uremic sarcopenia in chronic kidney disease. Sci Rep 2016;6:36618.
- [16] Aronov PA, Luo FJ, Plummer NS, Quan Z, Holmes S, Hostetter TH, et al. Colonic contribution to uremic solutes. J Am Soc Nephrol 2011;22:1769–76.
- [17] Mishima E, Fukuda S, Mukawa C, Yuri A, Kanemitsu Y, Matsumoto Y, et al. Evaluation of the impact of gut microbiota on uremic solute accumulation by a CE-TOFMS-based metabolomics approach. Kidney Int 2017;92:634–45.
- [18] Wikoff WR, Anfora AT, Liu J, Schultz PG, Lesley SA, Peters EC, et al. Metabolomics analysis reveals large effects of gut microflora on mammalian blood metabolites. Proc Natl Acad Sci USA 2009;106:3698–703.
- [19] Wang X, Yang S, Li S, Zhao L, Hao Y, Qin J, et al. Aberrant gut microbiota alters host metabolome and impacts renal failure in humans and rodents. Gut 2020;69:2131–42.
- [20] Liu J, Li B, Lee C, Zhu H, Zheng S, Pierro A. Protective effects of lactoferrin on injured intestinal epithelial cells. J Pediatr Surg 2019;54:2509–13.
- [21] Hao L, Shan Q, Wei J, Ma F, Sun P. Lactoferrin: major physiological functions and applications. Curr Protein & Peptide Sci 2019;20:139–44.
- [22] Hsu YH, Chiu IJ, Lin YF, Chen YJ, Lee YH, Chiu HW. Lactoferrin contributes a renoprotective effect in acute kidney injury and early renal fibrosis. Pharmaceutics 2020;12(5):434–48.
- [23] Garcia-Montoya IA, Cendon TS, Arevalo-Gallegos S, Rascon-Cruz Q. Lacto-ferrin a multiple bioactive protein: an overview. Biochim Biophys Acta 2012;1820;226–36.
- [24] Jang YS, Seo GY, Lee JM, Seo HY, Han HJ, Kim SJ, et al. Lactoferrin causes IgA and IgG2b isotype switching through betaglycan binding and activation of canonical TGF-beta signaling. Mucosal Immunol 2015;8:906–17.
- [25] Kang SH, Jin BR, Kim HJ, Seo GY, Jang YS, Kim SJ, et al. Lactoferrin combined with retinoic acid stimulates B1 cells to express IgA isotype and gut-homing molecules. Immune Net 2015;15:37–43.

- [26] Sherman MP, Bennett SH, Hwang FF, Yu C. Neonatal small bowel epithelia: enhancing anti-bacterial defense with lactoferrin and Lactobacillus GG. Biometals: An Int J Role Metal Ions Biol, Biochem Med 2004;17:285–9.
- [27] Kumakura S, Sato E, Sekimoto A, Hashizume Y, Yamakage S, Miyazaki M, et al. Nicotinamide attenuates the progression of renal failure in a mouse model of adenine-induced chronic kidney disease. Toxins (Basel) 2021;13:50.
- [28] Sato E, Tsunokuni Y, Kaneko M, Saigusa D, Saito R, Shimma S, et al. Metabolomics of a mouse model of preeclampsia induced by overexpressing soluble fms-like tyrosine kinase 1. Biochem Biophys Res Commun 2020:527-1064-71
- [29] Hosomi K, Ohno H, Murakami H, Natsume-Kitatani Y, Tanisawa K, Hirata S, et al. Method for preparing DNA from feces in guanidine thiocyanate solution affects 16S rRNA-based profiling of human microbiota diversity. Sci Rep 2017:7:4339.
- [30] Sato E, Hosomi K, Sekimoto A, Mishima E, Oe Y, Saigusa D, et al. Effects of the oral adsorbent AST-120 on fecal p-cresol and indole levels and on the gut microbiota composition. Biochem Biophys Res Commun 2020;525:773–9.
- [31] Buse MG, Weigand DA. Studies concerning the specificity of the effect of leucine on the turnover of proteins in muscles of control and diabetic rats. Biochim Biophys Acta 1977;475:81–9.
- [32] Kaspy MS, Hannaian SJ, Bell ZW, Churchward-Venne TA. The effects of branched-chain amino acids on muscle protein synthesis, muscle protein breakdown and associated molecular signalling responses in humans: an update. Nutr Res Rev 2024;37(2):273–86.
- [33] Bodine SC, Stitt TN, Gonzalez M, Kline WO, Stover GL, Bauerlein R, et al. Akt/mTOR pathway is a crucial regulator of skeletal muscle hypertrophy and can prevent muscle atrophy in vivo. Nat Cell Biol 2001;3:1014–19.
- [34] Egerman MA, Glass DJ. Signaling pathways controlling skeletal muscle mass. Crit Rev Biochem Molecul Biol 2014;49:59–68.
- [35] Toth MJ, Ades PA, Tischler MD, Tracy RP, LeWinter MM. Immune activation is associated with reduced skeletal muscle mass and physical function in chronic heart failure. Int J Cardiol 2006;109:179–87.
- [36] Thomson DM. The role of AMPK in the regulation of skeletal muscle size, hypertrophy, and regeneration. Int | Mol Sci 2018;19(10):3125-44.
- [37] Nakashima K, Ishida A. Regulation of autophagy in Chick myotubes: effects of insulin, insulin-like growth factor-I, and amino acids. J Poultry Sci 2018;55:257-62.
- [38] Barrett A,J., Kirschke H. Cathepsin B., Cathepsin H., and cathepsin L. Methods Enzymol. 1981;80 Pt C:535-61.
- [39] Stojanov S, Berlec A, Strukelj B. The influence of probiotics on the firmicutes/bacteroidetes ratio in the treatment of obesity and inflammatory bowel disease. Microorganisms 2020;8(11):1715–30.
- [40] He Q, Zhang LL, Li D, Wu J, Guo YX, Fan J, et al. Lactoferrin alleviates western diet-induced cognitive impairment through the microbiome-gut-brain axis. Curr Res Food Sci 2023;7:100533.
- [41] Sun J, Ren F, Xiong L, Zhao L, Guo H. Bovine lactoferrin suppresses high-fat diet induced obesity and modulates gut microbiota in C57BL/6J mice. J Function Foods 2016;22:189–200.

- [42] Li L, Ma C, Hurilebagen, Yuan H, Hu R, Wang W, et al. Effects of lactoferrin on intestinal flora of metabolic disorder mice. BMC Microbiol 2022;22:181–91.
- [43] Wang S, Zhou J, Xiao D, Shu G, Gu L. Bovine Lactoferrin protects dextran sulfate sodium salt mice against inflammation and impairment of colonic epithelial barrier by regulating gut microbial structure and metabolites. Front Nutr 2021;8:660598.
- [44] Mishima E, Fukuda S, Kanemitsu Y, Saigusa D, Mukawa C, Asaji K, et al. Canagliflozin reduces plasma uremic toxins and alters the intestinal microbiota composition in a chronic kidney disease mouse model. Am J Physiol Renal Physiol 2018;315:F824–FF33.
- [45] Mishima E, Fukuda S, Shima H, Hirayama A, Akiyama Y, Takeuchi Y, et al. Alteration of the intestinal environment by Lubiprostone is associated with amelioration of adenine-induced CKD. J Am Soc Nephrol 2014;26: 1787–1794.
- [46] Nanto-Hara F, Kanemitsu Y, Fukuda S, Kikuchi K, Asaji K, Saigusa D, et al. The guanylate cyclase C agonist linaclotide ameliorates the gut-cardio-renal axis in an adenine-induced mouse model of chronic kidney disease. Nephrol Dial Transplant 2020;35:250–64.
- [47] Iigo M, Kuhara T, Ushida Y, Sekine K, Moore MA, Tsuda H. Inhibitory effects of bovine lactoferrin on colon carcinoma 26 lung metastasis in mice. Clin Experiment Metastas 1999;17:35–40.
- [48] Cano NJ, Fouque D, Leverve XM. Application of branched-chain amino acids in human pathological states: renal failure. J Nutr 2006;136 299S–307S.
- [49] Shimizu N, Yoshikawa N, Ito N, Maruyama T, Suzuki Y, Takeda S, et al. Crosstalk between glucocorticoid receptor and nutritional sensor mTOR in skeletal muscle. Cell Metab 2011;13:170–82.
- [50] Paez HG, Pitzer CR, Alway SE. Age-related dysfunction in proteostasis and cellular quality control in the development of sarcopenia. Cells 2023;12(2):249-78.
- [51] Hickmann CE, Castanares-Zapatero D, Deldicque L, Van den Bergh P, Caty G, Robert A, et al. Impact of very early physical therapy during septic shock on skeletal muscle: a randomized controlled trial. Crit Care Med 2018;46:1436–43.
- [52] Penna F, Baccino FM, Costelli P. Coming back: autophagy in cachexia. Curr Opin Clin Nutr Metab Care 2014;17:241–6.
- [53] Ikeda M, Iijima H, Shinoda I, Iwamoto H, Takeda Y. Inhibitory effect of Bovine lactoferrin on catechol-O-methyltransferase. Molecules 2017;22(8):1373–84.
- [54] Troost FJ, Saris WH. Brummer RJ. Orally ingested human lactoferrin is digested and secreted in the upper gastrointestinal tract in vivo in women with ileostomies. J Nutr 2002;132:2597–600.
- [55] Drago-Serrano ME, Campos-Rodriguez R, Carrero JC, de la, Garza M. Lactoferrin and peptide-derivatives: antimicrobial agents with potential use in nonspecific immunity modulation. Current pharmaceutical design 2018;24: 1067-1078.
- [56] Zarzosa-Moreno D, Avalos-Gomez C, Ramirez-Texcalco LS, Torres-Lopez E, Ramirez-Mondragon R, Hernandez-Ramirez JO, et al. Lactoferrin and its derived peptides: an alternative for combating virulence mechanisms developed by pathogens. Molecules 2020;25(24):5763–810.